Journal of Theoretical Biology 260 (2009) 572–580

Contents lists available at ScienceDirect

Journal of Theoretical Biology

journal homepage: www.elsevier.com/locate/yjtbi

A model for hormonal control of the menstrual cycle: Structural consistency but sensitivity with regard to data

J.F. Selgrade [a,*], L.A. Harris [b], R.D. Pasteur [c]

[a] Department of Mathematics and Biomathematics Program, North Carolina State University, Raleigh, NC 27695, USA
[b] Department of Mathematics and Statistics, The College of New Jersey, Ewing, NJ 08628, USA
[c] Department of Mathematics and Computer Science, The College of Wooster, Wooster, OH 44691, USA

ARTICLE INFO

Article history:
Received 16 February 2009
Received in revised form
10 June 2009
Accepted 18 June 2009
Available online 25 June 2009

MSC:
92D25
39A11

Keywords:
Estradiol
Follicle
Parameter
Bifurcation

ABSTRACT

This study presents a 13-dimensional system of delayed differential equations which predicts serum concentrations of five hormones important for regulation of the menstrual cycle. Parameters for the system are fit to two different data sets for normally cycling women. For these best fit parameter sets, model simulations agree well with the two different data sets but one model also has an abnormal stable periodic solution, which may represent polycystic ovarian syndrome. This abnormal cycle occurs for the model in which the normal cycle has estradiol levels at the high end of the normal range. Differences in model behavior are explained by studying hysteresis curves in bifurcation diagrams with respect to sensitive model parameters. For instance, one sensitive parameter is indicative of the estradiol concentration that promotes pituitary synthesis of a large amount of luteinizing hormone, which is required for ovulation. Also, it is observed that models with greater early follicular growth rates may have a greater risk of cycling abnormally.

1. Introduction

Regulation of the human menstrual cycle depends on dual control via hormones synthesized by the hypothalamus and the pituitary glands and by the ovaries. A mechanistic, mathematical model for normally cycling women must capture this complicated interaction. Follicle stimulating hormone (*FSH*) and luteinizing hormone (*LH*) are secreted by the pituitary gland and control follicular development, ovulation and overall ovarian activity, see Hotchkiss and Knobil (1994), Yen (1999) and Zeleznik and Benyo (1994). The ovaries produce estradiol (E_2), progesterone (P_4) and inhibin (*Ih*) which influence the synthesis and release of *FSH* and *LH*.

A mathematical model for hormonal control of the menstrual cycle may be used to investigate cycle abnormalities such as polycystic ovarian syndrome (PCOS) (Yen, 1999a) and to simulate the effects of external hormone therapies on abnormally cycling women. Also, there is concern that environmental substances which have estrogenic activity may disrupt the normal cycle (Daston et al., 1997; McLachlan and Korach, 1995) and a mathematical model may be helpful in testing this hypothesis. Finally, oral contraception prevents the *LH* surge which is responsible for ovulation. Model simulations may be used to determine hormonal levels which will suppress this surge.

Various models for cycle regulation have been developed over the last 40 years, including Bogumil et al. (1972a), Bogumil et al. (1972b), McIntosh and McIntosh (1980), Plouffe and Luxenberg (1992) and Schwartz (1970). Recently, a 13-dimensional system of ordinary differential equations with discrete delays (Selgrade and Schlosser, 1999; Schlosser and Selgrade, 2000; Harris-Clark et al., 2003) describing the concentrations of these five hormones has predicted blood levels of these hormones which agree with data in the literature for normally cycling women (McLachlan et al., 1990). Reinecke and Deuflhard (2007), use a system of 43 delay differential equations to extend the Harris-Clark et al. model to include additional biological factors. Their model has a stochastic component for the gonadotropin releasing hormone (*GnRH*) pulse generator and detailed equations for *LH* and *FSH* receptor binding and synthesis of hormones in the ovary.

Harris-Clark et al. (2003) estimated the parameters in their system using the data in McLachlan et al. (1990), for 33 normally cycling women. These data are daily averages of the five hormones for 31 consecutive days and the averages are computed by centering data from each individual woman about the day of her *LH* surge. The E_2 data in McLachlan et al. (1990) are given by the

* Corresponding author. Tel.: +1 919 515 8589; fax: +1 919 515 3798.
E-mail addresses: selgrade@math.ncsu.edu (J.F. Selgrade), harrisl@tcnj.edu (L.A. Harris), rpasteur@wooster.edu (R.D. Pasteur).

0022-5193/$ - see front matter © 2009 Elsevier Ltd. All rights reserved.
doi:10.1016/j.jtbi.2009.06.017

open circles in Fig. 1. Model parameters were estimated from the McLachlan data and model simulations (Harris-Clark et al., 2003) closely approximated these data (see Fig. 2(a) for the graph of E_2). We refer to the model with this parameter set as the McLachlan model. Welt et al. (1999), presented data for these five hormones (inhibin A replacing inhibin) from 23 normally cycling women for a 28 day period and these E_2 data are depicted by closed circles in Fig. 1. Clearly the mid-cycle peak in E_2 for the Welt data is lower than that for the McLachlan data by approximately 20% and the luteal peak is also lower. Pasteur (2008) fit the same system to the Welt data, which are a bit noisier than the McLachlan data and differ in units for some hormones. Model simulations (referred to as the Welt model) are good fits to the Welt data, e.g., see the graph of E_2 in Fig. 2(b).

The dynamical behavior of the McLachlan model has some differences from the Welt model. Most importantly, the McLachlan model has two stable periodic solutions (Harris-Clark et al., 2003)—one fits the McLachlan data for normally cycling women and the other is anovulatory (see the dashed curves in Fig. 4) and may represent PCOS because of a low P_4 concentration and an acyclic (fluctuates very little during the month) E_2 concentration (Yen, 1999a). By contrast, the Welt model has only one stable periodic solution and it fits the Welt data for normally cycling women. Such a discrepancy in dynamical behavior could suggest a lack of consistency in this model for cycle regulation. Here we show that this is not the case by analyzing bifurcation diagrams with respect to sensitive parameters and by displaying hysteresis loops which explain model differences. Hence, both models have similar dynamical structures but exhibit different asymptotic behaviors due to parameter sensitivity which manifests itself when slightly different data sets are used to estimate parameters. This observation indicates the importance of understanding broader model behavior beyond the specific simulations corresponding to one parameter set if a modeler wishes to use the model to make biological conclusions. For the menstrual cycle model studied here, we also notice that the higher E_2 profile corresponds to the model displaying an abnormal cycle. Is this biologically significant, i.e., does a woman with E_2 levels at the high end of the normal range have a greater chance of cycling abnormally? We return to this question in Section 5.

In this paper, Section 2 discusses model background and development. In Section 3, we compare simulation results of the McLachlan model and the Welt model. Sensitivity analysis, which is done in Section 4, orders the most sensitive parameters and shows they are the same for both models. Sections 5 and 6 display and compare bifurcation diagrams and investigate structural consistency. Section 7 summarizes the results.

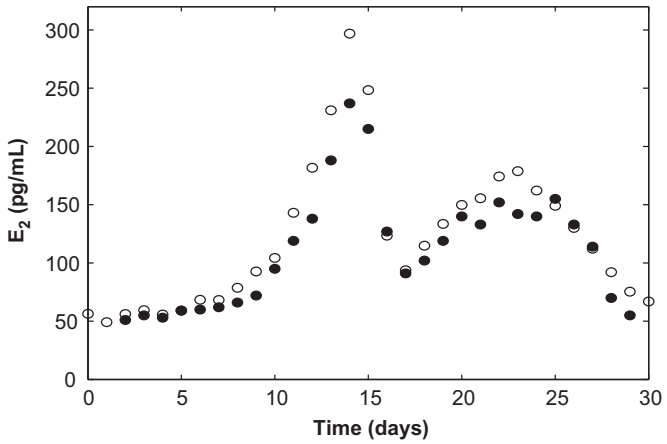

Fig. 1. Estradiol (E_2) data from McLachlan et al. (1990) (31 open circles) and from Welt et al. (1999) (28 closed circles). The Welt data are translated to the right by 2 days so the time of the mid-cycle E_2 peak agrees with that of the McLachlan data.

2. Background and model structure

The menstrual cycle for normal adult females consists of two phases, the follicular phase and the luteal phase, separated by ovulation (Ojeda, 1992). The pituitary, influenced by signals from the hypothalamus, synthesizes and releases the gonadotropin hormones, *FSH* and *LH*. These hormones have a pulsatile secretion pattern. However, we assume that the ovary responds to average blood levels of *FSH* and *LH* (Odell, 1979), so we track their average concentrations in the blood. In response to the gonadotropin hormones, the ovaries produce E_2, $P_4$and *Ih*. In turn, the ovarian hormones affect the pituitary's synthesis and release of *FSH* and

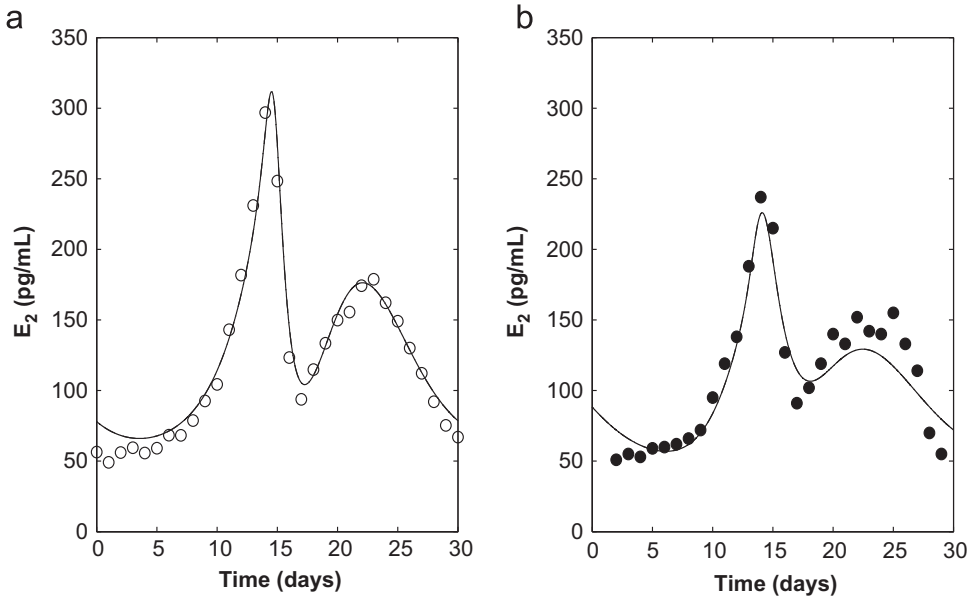

Fig. 2. (a) E_2 data from McLachlan et al. (1990) and McLachlan model simulation (solid curve); (b) E_2 data from Welt et al. (1999) and Welt model simulation (solid curve).

LH during the various stages of the cycle. Because of this dual control, the modeling procedure is divided into three steps.

In the first step, the synthesis, release and clearance of the gonadotropin hormones are described by two two-dimensional systems of differential equations (S1)–(S4), which contain specific input functions of time t for the ovarian hormones $E_2(t), P_4(t)$ and $Ih(t)$ constructed using data from the biological literature (McLachlan et al., 1990; Welt et al., 1999). The state variables are the amount of gonadotropin hormone in the pituitary's releasable pool, *RP*, and the serum concentration of that hormone. As explained in Schlosser and Selgrade (2000), the model assumes that E_2 inhibits hormone release but, after E_2 reaches a threshold level, E_2 stimulates *LH* synthesis. The synthesis terms in (S1) and (S3) contain time lags in the ovarian hormones to account for delayed effects on the synthesis rates of the gonadotropin hormones. The only known parameters are clearance rates for *LH* and *FSH* and blood volume v. To estimate the nine unknown parameters of the *LH* system (S1) and (S2) and the six unknown parameters of the *FSH* system (S3) and (S4), Harris-Clark et al. (2003) and Pasteur (2008) employed the Nelder–Mead method in MATLAB to minimize least squares cost functions which used the *LH* data for (S1) and (S2) and the *FSH* data for (S3) and (S4). Parameter estimates from previous work (Schlosser and Selgrade, 2000) and some manual parameter adjustments were needed to get reasonable starting parameter sets because the Nelder–Mead method is a local minimizer.

Secondly, as derived in Selgrade and Schlosser (1999) there is a nine-dimensional system of differential equations (S5)–(S13) for nine stages of the monthly development of the ovary. These stages represent the active capacities of follicular and luteal tissue to produce hormones under the influence of the gonadotropin hormones. The follicular phase is divided into three stages referred to as the menstrual follicular stage *MsF*, the secondary follicular stage *SeF* and the primary follicular stage *PrF*. Ovulation is represented by two scars, Sc_1 and Sc_2, and the luteal phase consists of four stages, Lut_i for $i = 1, \ldots, 4$. The gonadotropins promote the growth of each stage and the transition from one stage to the next as indicated in Fig. 3. Clearance from the blood of the ovarian hormones is very rapid compared with clearance of the pituitary hormones. Hence, in agreement with Bogumil et al. (1972a), we assume that serum levels of E_2, $P_4$and *Ih* are at quasi-steady state (Keener and Sneyd, 2009) and take these concentrations to be linear combinations of appropriate ovarian stages, see (A1)–(A3). Into (S5)–(S13), we inserted explicit functions of t constructed from the data for *LH* and *FSH*. Then parameter identification was done in either of two ways.

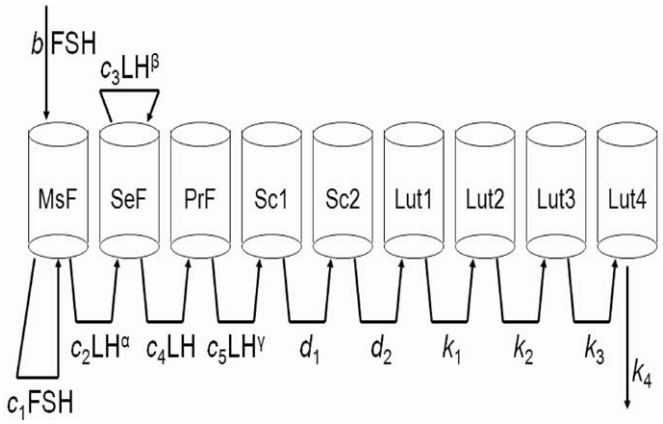

Fig. 3. Diagram of the ovarian stages where compartments represent follicular or luteal tissue. Arrows indicate transition from one stage to the next stage or growth within a stage.

Harris-Clark et al. (2003) estimated the 19 parameters in (S5)–(S13) and (A1) using a least squares cost function with the E_2 data and, then, estimated the seven parameters in (A2) and (A3) using cost functions with the P_4 and the *Ih* data. On the other hand, Pasteur (2008) estimated all 26 parameters using one weighted cost function, which scaled the ovarian hormones to the same order of magnitude.

The final step merges the pituitary and ovarian components into a 13-dimensional system of delayed, ordinary differential equations (S1)–(S13) with auxiliary equations (A1)–(A3). The state variables for (S1)–(S13) are RP_{LH}, *LH*, RP_{FSH}, *FSH* and the nine ovarian variables indicated by the compartments in Fig. 3. Starting with the parameter values obtained in the preceding two steps, additional parameter refinements were performed to improve fits to data. Thus, 44 parameters for the McLachlan model (Harris-Clark et al., 2003) and for the Welt model (Pasteur, 2008) were identified.

System (S)

$$\frac{d}{dt}RP_{LH} = \frac{V_{0,LH} + \dfrac{V_{1,LH}E_2(t-d_E)^8}{Km_{LH}^8 + E_2(t-d_E)^8}}{1 + P_4(t-d_P)/Ki_{LH,P}} - \frac{k_{LH}[1 + c_{LH,P}P_4]RP_{LH}}{1 + c_{LH,E}E_2} \tag{S1}$$

$$\frac{d}{dt}LH = \frac{1}{v}\frac{k_{LH}[1 + c_{LH,P}P_4]RP_{LH}}{1 + c_{LH,E}E_2} - a_{LH}\,LH \tag{S2}$$

$$\frac{d}{dt}RP_{FSH} = \frac{V_{FSH}}{1 + Ih(t-d_{Ih})/Ki_{FSH,Ih}} - \frac{k_{FSH}[1 + c_{FSH,P}P_4]RP_{FSH}}{1 + c_{FSH,E}E_2^2} \tag{S3}$$

$$\frac{d}{dt}FSH = \frac{1}{v}\frac{k_{FSH}[1 + c_{FSH,P}P_4]RP_{FSH}}{1 + c_{FSH,E}E_2^2} - a_{FSH}\,FSH \tag{S4}$$

$$\frac{d}{dt}MsF = bFSH + [c_1\ FSH - c_2 LH^{\alpha}]\,MsF \tag{S5}$$

$$\frac{d}{dt}SeF = c_2\,LH^{\alpha}\,MsF + [c_3\,LH^{\beta} - c_4\,LH]\,SeF \tag{S6}$$

$$\frac{d}{dt}PrF = c_4\,LH\,SeF - c_5\,LH^{\gamma}\,PrF \tag{S7}$$

$$\frac{d}{dt}Sc_1 = c_5\,LH^{\gamma}\,PrF - d_1\,Sc_1 \tag{S8}$$

$$\frac{d}{dt}Sc_2 = d_1\,Sc_1 - d_2\,Sc_2 \tag{S9}$$

$$\frac{d}{dt}Lut_1 = d_2\,Sc_2 - k_1\,Lut_1 \tag{S10}$$

$$\frac{d}{dt}Lut_2 = k_1\,Lut_1 - k_2\,Lut_2 \tag{S11}$$

$$\frac{d}{dt}Lut_3 = k_2\,Lut_2 - k_3\,Lut_3 \tag{S12}$$

$$\frac{d}{dt}Lut_4 = k_3\,Lut_3 - k_4\,Lut_4 \tag{S13}$$

The following three auxiliary equations (A) give serum levels of E_2, P_4 and *Ih*, as functions of the appropriate state variables, which appear in system (S):

Auxiliary equations (A)

$$E_2 = e_0 + e_1 SeF + e_2 PrF + e_3 Lut_4 \tag{A1}$$

$$P_4 = p_0 + p_1 Lut_3 + p_2 Lut_4 \tag{A2}$$

$$Ih = h_0 + h_1 PrF + h_2 Lut_3 + h_3 Lut_4 \tag{A3}$$

Because of the form of (A), a function which represents an external ovarian hormone may be added to the right side of (A). Hence, numerical simulations may be used to test the effects of exogenous ovarian hormones on model behavior.

3. Results for McLachlan model and Welt model

Simulations of the McLachlan model for system (S) are discussed in detail in Harris-Clark et al. (2003). There are two locally asymptotically stable periodic solutions. One solution has a period of 29.5 days and approximates the McLachlan data for normally cycling women (see the solid curves in Fig. 4 for E_2 and LH) and the other solution has period 24 days and represents an abnormal cycle (see the dashed curves in Fig. 4). Because there is no LH surge, the abnormal cycle is anovulatory and its acyclic E_2 profile suggests the possibility of PCOS (Yen, 1999a). Although the domain of attraction of the normal cycle appears to be much larger than that of the abnormal cycle, Harris-Clark et al. (2003) showed that a carefully timed transient E_2 perturbation applied to the normal cycle could result in the system cycling abnormally. Conversely, the transient addition of external P_4 was shown to perturb an abnormal cycle back into the normal range (Harris-Clark et al., 2003).

Simulations of the Welt model (Pasteur, 2008) revealed only one stable periodic solution, see Fig. 5. It has a period of 28 days and approximates the Welt data set of 28 points. Observe that the LH units for the Welt data are different from those of the McLachlan data. After transient perturbations, the Welt model always returns to the unique stable cycle but possibly out of phase.

The only difference between the McLachlan model and the Welt model is in the parameters which fit the two data sets. However, because of a different number of stable periodic solutions, the McLachlan model and the Welt model predict different behavior for our menstrual cycle regulation model, (S) with (A). Depending on initial hormone concentrations, a woman described by the McLachlan model may cycle normally or abnormally. On the other hand, a woman described by the Welt model cycles normally regardless of initial conditions. It is reasonable to suggest that changes in parameters for the Welt model may yield a parameter set still different from the McLachlan model but having two stable cycles. In fact, we show that varying just the parameter Km_{LH} in the LH synthesis term in (S1) has this effect. One reason for choosing Km_{LH} for this analysis is that model behavior is sensitive to variations in Km_{LH}.

4. Sensitivity analysis

Normalized sensitivity coefficients measure the effect of small variations in parameters on system outputs. Roughly speaking, this coefficient is a partial derivative of a function of the state variables with respect to a parameter, normalized so that comparisons may be made among variables and parameters. Specifically, the coefficient is a discrete change in the system output relative to the output value divided by the change in the parameter relative to the parameter value. For instance, if the parameter p is increased by 1% and the system output is denoted

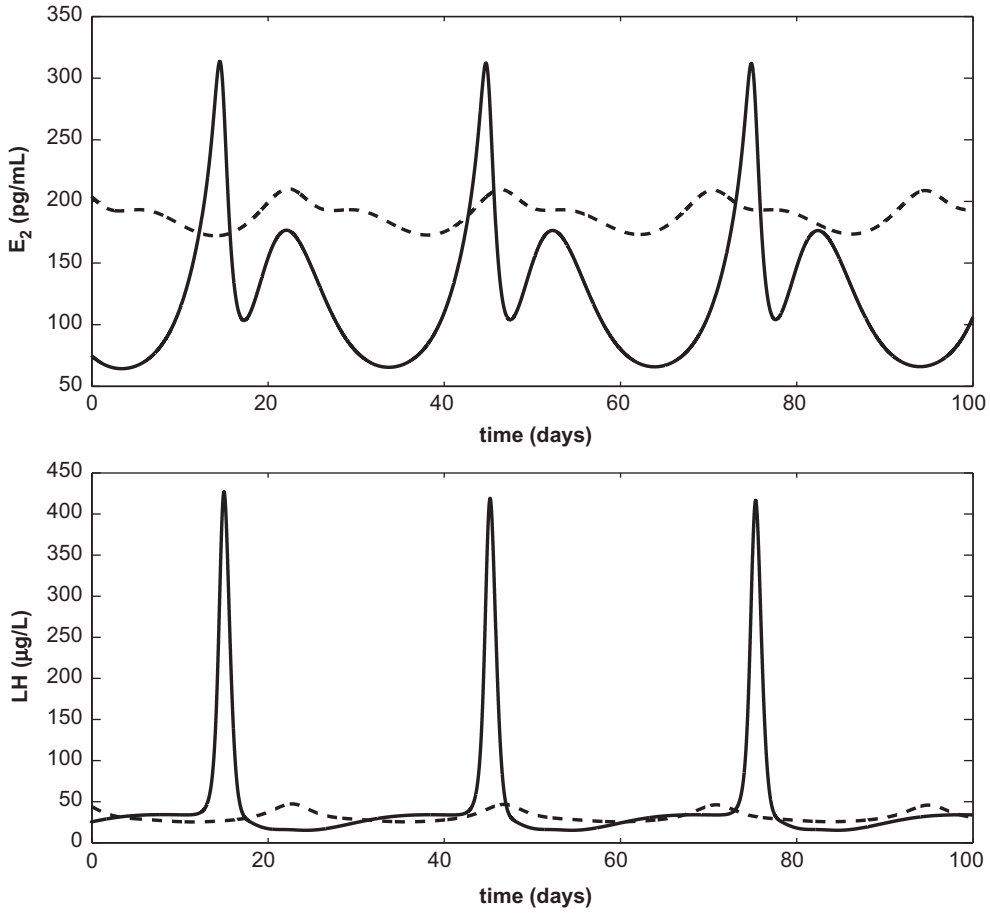

Fig. 4. E_2 and LH simulations of the McLachlan model. The solid curves depict a normal cycle and the dashed curves, an abnormal cycle.

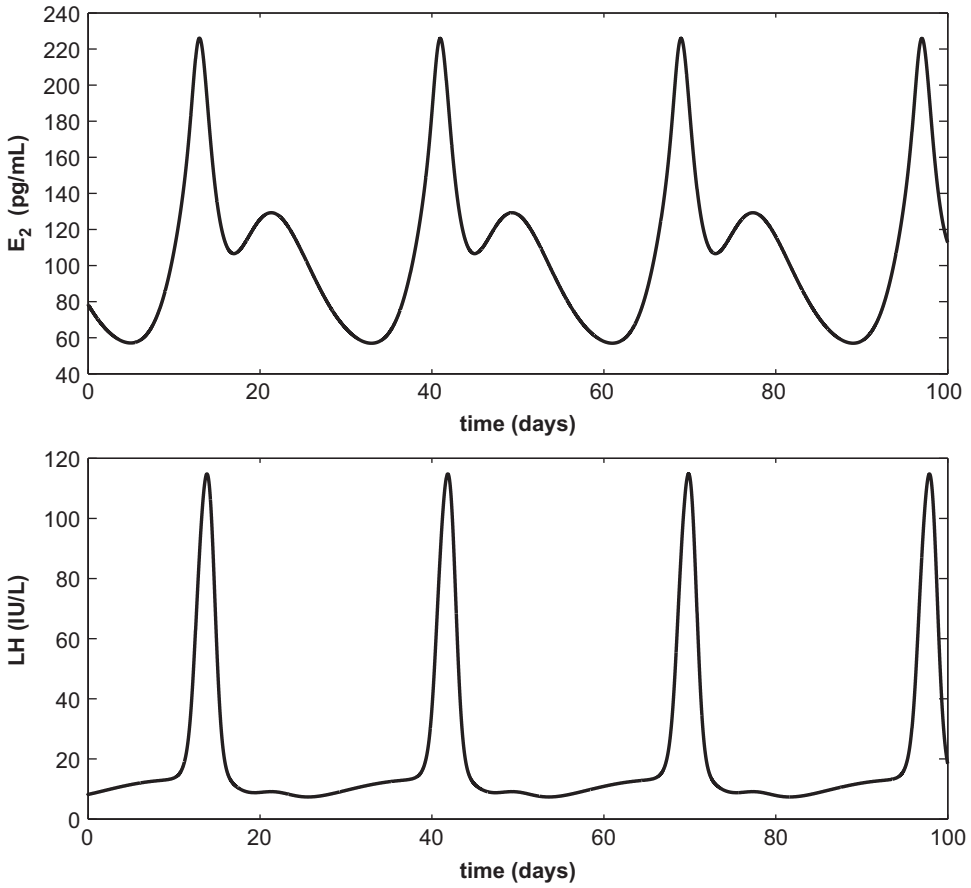

Fig. 5. E_2 and LH simulations of the Welt model.

as a function of p by $SO(p)$ then the normalized sensitivity coefficient is computed according to the formula

$$\frac{\Delta SO}{SO}\frac{p}{\Delta p}=\frac{SO(1.01p)-SO(p)}{SO(p)}\frac{p}{0.01p}=100\frac{SO(1.01p)-SO(p)}{SO(p)} \quad (4.1)$$

During the menstrual cycle, a significant follicular phase rise in E_2 stimulates the secretion of LH and causes the LH surge, which is necessary for ovulation and normal ovarian function. Also, our primary point of comparison between the two data sets is the difference in E_2 mid-cycle peaks. Hence, for our sensitivity analysis, the system output we measure is the height of the E_2 mid-cycle peak along the normal cycle for both the McLachlan model and the Welt model. We use formula (4.1) to compute sensitivity coefficients for the 44 parameters. The six most sensitive with respect to the E_2 mid-cycle peak are the same for both models. Table 1 lists parameter values and the sensitivity coefficients for these six most sensitive parameters ordered by the absolute value of the entry in the last column, i.e., the sensitivity coefficient for the Welt model. A negative coefficient means that the E_2 mid-cycle peak decreases as the parameter increases. Notice that the McLachlan model is more sensitive to parameter variation than the Welt model. Although the most sensitive parameter is the LH exponent α in (S5) and (S6), we focus on the second most sensitive parameter Km_{LH} because of its physiological significance.

Table 1
E_2 peak normalized sensitivity coeffs. for six most sensitive parameters.

Par.	Definition	McLachlan value	coeff.	Welt value	coeff.
α	LH exponent	0.7736	−6.72	0.79	−1.78
Km_{LH}	Half-saturation	360 pg/mL	1.19	180 pg/mL	0.90
c_2	MsF transfer	0.048 (L/μg)$^\alpha$/day	−2.2	0.09 (L/IU)$^\alpha$/day	−0.83
V_{FSH}	FSH growth	5700 μg/day	2.25	375 IU/day	0.74
c_1	MsF growth	0.0058 L/μg/day	2.34	0.09 L/IU/day	0.74
$V_{0,LH}$	LH growth	1263.4 μg/day	−1.62	500 IU/day	−0.65

5. Comparison of bifurcation diagrams

The rate of LH synthesis increases with E_2 serum concentration according to the rational function (Hill function) in the numerator of the first term of (S1) because the denominator is almost constant during the follicular phase. This Hill function is a sigmoid shaped curve which determines a sharp transition from a low synthesis rate given by $V_{0,LH}$ to a maximal rate (saturation) given by $V_{1,LH}$. The parameter Km_{LH} is the value of E_2 where the Hill function reaches half-saturation and where the curve is steep (slope proportional to $V_{1,LH}$). When E_2 reaches the value of Km_{LH}, the pituitary is synthesizing substantial amounts of LH. In fact, for the McLachlan model LH synthesis is considerable even for E_2 levels less than Km_{LH} because the parameter $V_{1,LH}=91\,000$ μg/day is large (see Schlosser and Selgrade, 2000, for details). Also, Table 1 indicates that the E_2 peak is sensitive to variation in Km_{LH}. Hence, we investigate how model behavior is affected by changes in Km_{LH}, i.e., we look for bifurcations with respect to the parameter Km_{LH}.

Figs. 6, 8 and 10 illustrate the bifurcation curves for system (S) where the vertical axis denotes the difference between the maximum and the minimum of the first state variable, RP_{LH}, along a periodic solution to (S) and, hence, this difference is a measure of the amplitude of the periodic solution. At an

equilibrium this difference is zero, so the horizontal axis denotes an equilibrium. Because system (S) consists of delay equations and there are ranges of parameter values where there exist three periodic solutions of widely varying amplitudes, tracking all of the solutions is difficult, particularly for unstable solutions. Hence, we developed and programmed in MATLAB a tedious method of careful shooting to obtain the positions of stable and unstable periodic solutions. At any fixed value of Km_{LH} for which there are two stable periodic solutions, it was possible to obtain a solution attracted toward either of these stable cycles by varying only the initial condition corresponding to the first ovarian compartment, *MsF*. By repeated simulations, we estimated the branch value corresponding to this initial condition for which slight perturbations to the initial condition lead to observing the two distinct stable periodic solutions. When using an initial condition that was very close to the initial condition that produced this branch value, we observed a transient approximation of the unstable periodic solution, potentially lasting for many cycles, before eventual visible attraction to one of the stable solutions occurred. This enabled estimation of the period, amplitude and profile associated with the unstable periodic solution at a given value of Km_{LH}, as in Fig. 7. Because they are attracting, the stable cycles were easier to track. Repeating the same process with other values of Km_{LH} resulted in the bifurcation curves of Figs. 6, 8 and 10.

Fig. 6 gives the bifurcation diagram for the Welt model. $Km_{LH} = 180$ pg/mL is the parameter value in the parameter set which fits the Welt data best, so the normal cycle is denoted by the $*$ in the figure. For small values of Km_{LH}, the only stable solution is an equilibrium. At $Km_{LH} \approx 68.66$, a Hopf bifurcation (HB in Fig. 6) occurs which results in a stable periodic solution (solid curve) and an unstable equilibrium (dotted horizontal axis). This stable cycle continues to the large amplitude (normal) cycle as Km_{LH} increases to 180. Then when $Km_{LH} \approx 246.1$, a saddle-node (SN) bifurcation (not labeled) occurs resulting in a small amplitude stable cycle (solid curve) and an unstable cycle (dotted curve) as indicated in Fig. 6. The small amplitude cycle quickly disappears via another Hopf bifurcation at $Km_{LH} \approx 256.9$. The unstable cycle coalesces with the continuation of the Welt model normal cycle in a saddle-node bifurcation at $Km_{LH} \approx 308.2$ and both disappear (see SN in Fig. 6). For $Km_{LH} > 308.2$, only a stable equilibrium remains. The sigmoid shaped curve on the right in Fig. 6 which contains stable and unstable cycles is referred to as a hysteresis curve or loop. For Km_{LH} between 246.1 and 256.9, there are two stable cycles and

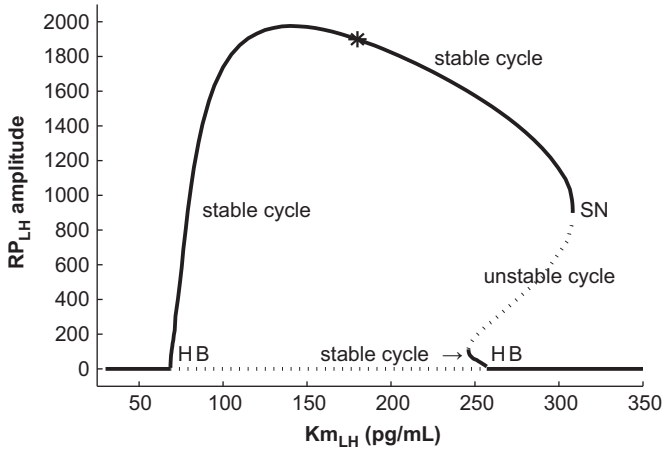

Fig. 6. Bifurcation diagram for Welt model with respect to Km_{LH}. HB and SN denote Hopf and saddle-node bifurcations. Solid curves denote stable solutions and dotted curves, unstable solutions. The $*$ indicates the position of the normal cycle for the Welt model and this cycle is the only stable solution at $Km_{LH} = 180$ pg/mL.

an unstable cycle, which are depicted in Fig. 7 for $Km_{LH} = 250$. Notice the similarity between the two stable cycles in Fig. 7 and the E_2 profiles of the two stable cycles for the McLachlan model (Fig. 4). In particular, E_2 levels of the large amplitude cycles in both graphs reach 300 pg/mL at mid-cycle.

Fig. 8, the bifurcation curve for the McLachlan model, depicts a closed loop of stable and unstable cycles because of two saddle-nodes at $Km_{LH} \approx 270$ and 770. The upper half of the loop represents stable cycles and the lower half represents unstable cycles. Also there is a Hopf bifurcation at $Km_{LH} \approx 265$ resulting in a stable cycle of small amplitude which persists until at least $Km_{LH} \approx 1500$, where it disappears in another Hopf bifurcation (not shown). Three vertical phase lines are drawn in Fig. 8 to indicate the directions of solution curves toward attracting solutions or away from unstable solutions. The line at $Km_{LH} = 150$ depicts solutions that approach the stable equilibrium represented by the point on the horizontal axis. Because SN denotes a degenerate periodic solution, the line through SN contains solutions that approach SN and solutions that leave SN and approach the small amplitude stable cycle. The line at $Km_{LH} = 400$ depicts solutions that approach the two stable cycles and solutions that leave the unstable cycle and the unstable equilibrium. $Km_{LH} = 360$ corresponds to the parameter set that fits best the McLachlan data and is indicated by a $*$ in Fig. 8. This parameter value lies between the saddle-nodes and between the Hopf bifurcations. Hence, a woman cycling according to the McLachlan data (i.e., the McLachlan model) has the possibility of cycling normally or abnormally depending on initial hormone concentrations. In fact, the possibility of dual cycles exists for any Km_{LH} value between 270 and 770. The smaller amplitude stable cycle is anovulatory because the amount of RP_{LH} is too low to permit a *LH* surge. If Km_{LH} is outside this range, i.e., far enough to the left or to the right in the diagram, then the woman will have only an anovulatory cycle.

By contrast, for the Welt model, the best fit parameter value $Km_{LH} = 180$ lies to the left of the hysteresis curve in Fig. 6 and so a woman cycling according to the Welt model will only cycle normally. From Fig. 2, it is clear that E_2 levels for the Welt model are lower than those for the McLachlan model and reach only 240 pg/mL at mid-cycle compared to 300 pg/mL. However, as Km_{LH} increases from 180, the E_2 profile for the Welt model changes and becomes quite similar to the E_2 profile of the McLachlan model (Fig. 9). As predicted by Table 1, as Km_{LH} increases, the Welt model mid-cycle E_2 increases and reaches $E_2 \approx 300$ pg/mL when $Km_{LH} = 250$. But at this value of Km_{LH}, the Welt model also admits the abnormal cycle shown in Figs. 6 and 7. Hence, a woman cycling normally with a high E_2 profile (either graph in Fig. 9) has the possibility of being perturbed into an abnormal, anovulatory cycle. As far as we know, this hypothesis has not been tested experimentally. In this regard, a clinical approach might be to compare E_2 levels of normally cycling women with those of PCOS patients who cycle normally after successful therapy to see if the post-PCOS E_2 profiles peaks are higher than those of normal women.

6. Bifurcation diagrams for different follicle growth rates

The bifurcation diagrams, Figs. 6 and 8, appear quite different. From Table 1, we see that the E_2 peak is sensitive to the ovarian growth parameter c_2, which transfers mass from the first follicular stage *MsF* to the second follicular stage *SeF* (S5) and (S6). For the McLachlan model, the normal cycle occurs when $c_2 = 0.048$. The bifurcation diagram (Fig. 8) is drawn for that c_2 value. If analogous bifurcation diagrams are drawn for smaller c_2 values, the closed loop in Fig. 8 develops a gap and bifurcation diagrams become

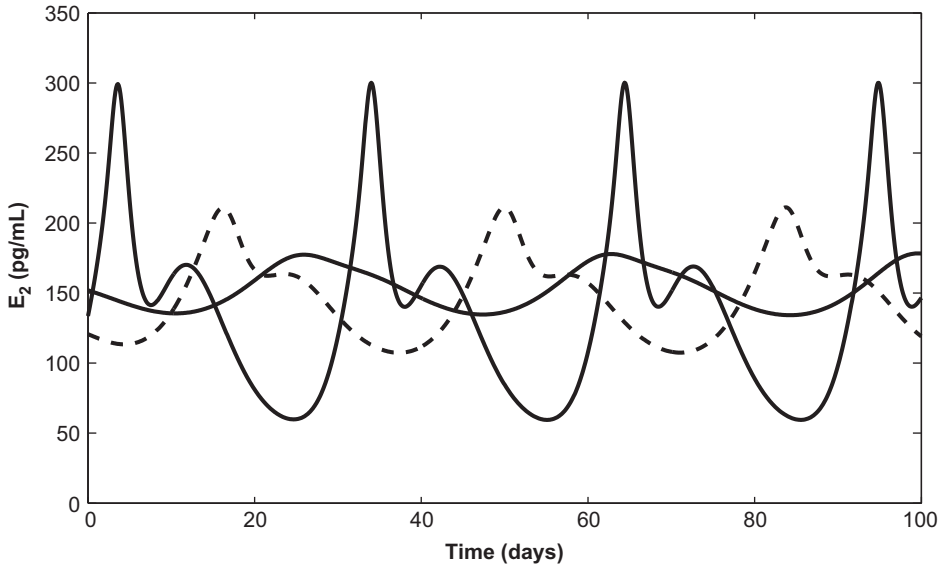

Fig. 7. Graphs of the E_2 profiles for three cycles of the Welt model when $Km_{LH} = 250$. The solid curves are stable cycles and the dashed curve is an unstable cycle.

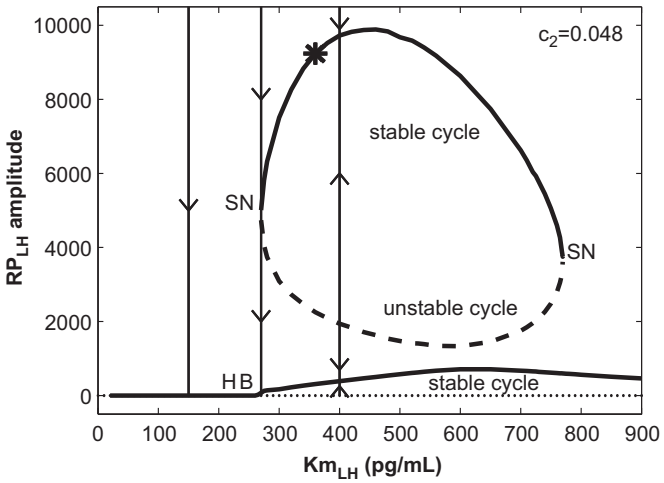

Fig. 8. Bifurcation diagram for McLachlan model with respect to Km_{LH}. HB and SN denote Hopf and saddle-node bifurcations. Solid curves denote stable solutions and dotted or dashed curves denote unstable solutions. The $*$ indicates the position of the normal cycle for the McLachlan model. Vertical phase lines and arrows represent the directions of solution curves for Km_{LH} values near HB and SN.

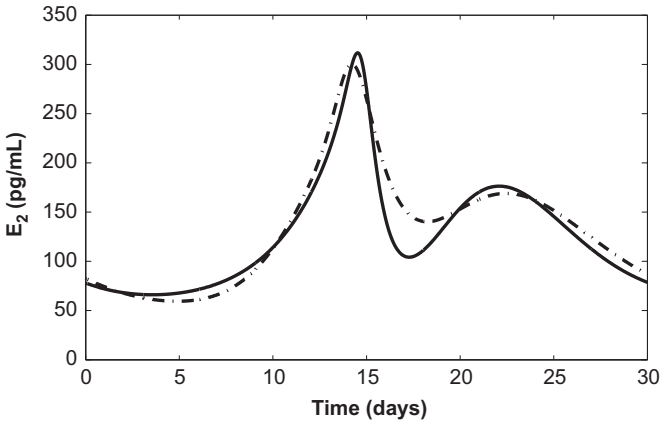

Fig. 9. Graph of the E_2 profile for the McLachlan model when $Km_{LH} = 360$ pg/mL (solid curve) and E_2 for the Welt model when $Km_{LH} = 250$ pg/mL (dashed curve).

somewhat similar to the Welt diagram Fig. 6. Specifically, as c_2 decreases, the closed loop moves down toward the curve of abnormal cycles, touches this curve in what appears to be a transcritical bifurcation in the parameter Km_{LH} and then breaks to form two new saddle-node bifurcations (see Fig. 10). Fig. 10(a) depicts the bifurcation diagram for the McLachlan model when $c_2 = 0.047$. An interval of Km_{LH} values has formed between the two SN's for which there are no abnormal cycles. As c_2 decreases to 0.045, this interval of Km_{LH} values increases (Fig. 10(b)) and, hence, the likelihood of abnormal cycling has diminished. However, the Km_{LH} value of 360 pg/mL, which corresponds to the McLachlan data, still lies in the Km_{LH} parameter range where there are two stable cycles (Fig. 10). Numerical simulations of (S) with $Km_{LH} = 360$ indicate that decreasing c_2 permits slightly more growth of the *MsF* follicular stage before mass transfer occurs to the next stage *SeF*. A greater *MsF* mass compensates for a smaller c_2 value in (S6) and results in more *SeF*, which is somewhat unexpected. In turn, more *SeF* mass results in slightly more follicular E_2 via (A1) and a slightly earlier and higher *LH* surge. In this model, early cycle follicular development appears sensitive to the interplay between ovarian state variables and parameters. Successful modeling of early follicular development may require additional ovarian stages which capture the transition in the ovaries from the late luteal phase of one cycle to the early follicular phase of the next cycle. To investigate this transition in the future we will use a 12 stage ovarian model (Pasteur, 2008), which includes two new stages representing pre-antral and early antral follicles (Odell, 1979; Ojeda, 1992).

7. Summary and conclusion

This study compares the dynamical behavior of two models of cycle regulation given by the same system of differential equations (S) but based on two different data sets (McLachlan et al., 1990; Welt et al., 1999) for the same five hormones. The McLachlan model has two stable periodic solutions, a normal cycle and an abnormal cycle possibly representing PCOS, and the Welt model has only one stable periodic solution. We show that this apparent lack of consistency may be explained by analyzing bifurcation diagrams with respect to the half-saturation parameter Km_{LH} in the *LH* synthesis term (S1) and a follicular mass

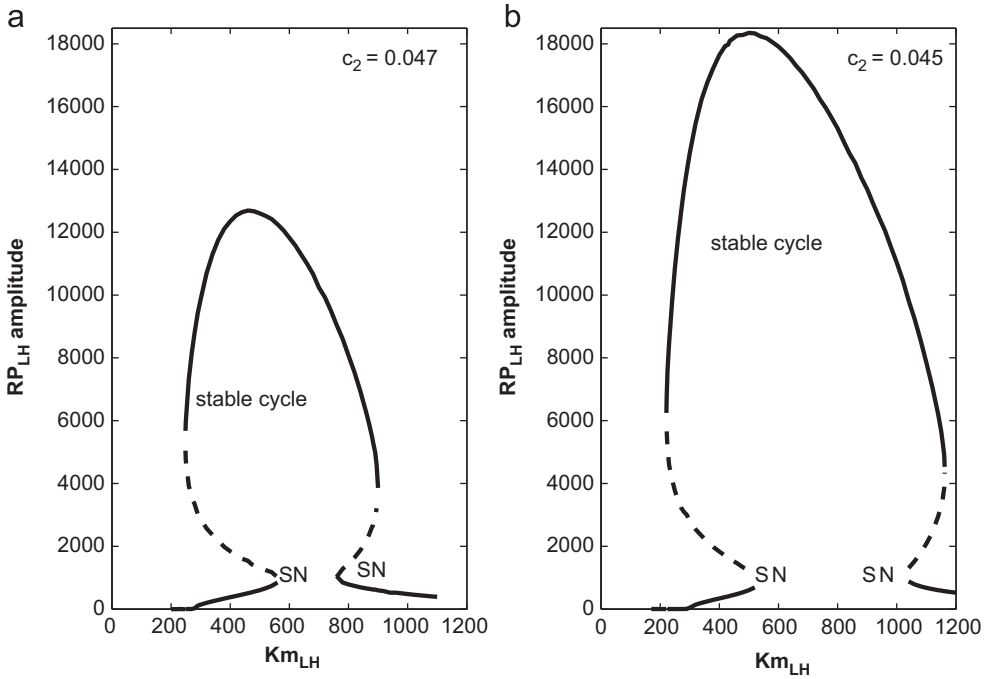

Fig. 10. (a) McLachlan model, $c_2 = 0.047$; (b) McLachlan model, $c_2 = 0.045$.

transfer coefficient c_2 (S5) and (S6). Km_{LH} is a measure of the level of estradiol for which the pituitary synthesizes a large amount of *LH* and, hence, for the *LH* surge and ovulation to occur. The McLachlan Km_{LH} value lies within a bifurcation loop (Fig. 8), which results in the existence of the two stable cycles, but the parameter value for the Welt model lies outside the hysteresis loop in the corresponding Welt bifurcation diagram (Fig. 6). If the Welt Km_{LH} parameter is increased to a position within the hysteresis loop not only does the Welt model have an abnormal cycle but the new Welt E_2 profile is very similar to that of the McLachlan model (see Fig. 9), although the Km_{LH} values are different. This similarity in conjunction with the presence of an abnormal cycle may indicate that a woman with E_2 levels at the upper end of the normal range has a greater risk of cycling abnormally. This hypothesis should be investigated clinically. Generally, understanding variations in model behavior due to changes in sensitive parameters may help a modeler make biological conclusions from model behavior and may suggest directions for future biological investigation.

The abnormal cycle exhibits an acyclic E_2 profile (Fig. 4) and, hence, high E_2 levels during the early follicular phase of the cycle. *In vivo*, this E_2 is secreted by an excess of early antral follicles, which is a characteristic of PCOS (Jonard et al., 2003; Pigny et al., 2006; Chen et al., 2008). Understanding early follicular development will require refinements of the present 13-dimensional model which include the late luteal to early follicular transition and will require the consideration of other factors such as androgen levels and insulin resistance.

Acknowledgments

Some of the research results reported here are from unpublished portions of the doctoral thesis of Pasteur (2008) and of the doctoral thesis of Harris (2001), who was supported by a fellowship from the National Physical Science Consortium. The authors would like to thank Claude L. Hughes for helpful conversations and two anonymous reviewers whose suggestions improved the paper.

References

Bogumil, R.J., Ferin, M., Rootenberg, J., Speroff, L., Vande Wiele, R.L., 1972a. Mathematical studies of the human menstrual cycle. I: Formulation of a mathematical model. J. Clin. Endocrinol. Metab. 35, 126–143.

Bogumil, R.J., Ferin, M., Vande Wiele, R.L., 1972b. Mathematical studies of the human menstrual cycle. II: Simulation performance of a model of the human menstrual cycle. J. Clin. Endocrinol. Metab. 35, 144–156.

Chen, M.-J., Yang, W.-S., Chen, C.-L., Wu, M.-Y., Yang, Y.-S., Ho, H.-N., 2008. The relationship between anti-Müllerian hormone, androgen and insulin resistance on the number of antral follicles in women with polycystic ovary syndrome. Hum. Reprod. 23, 952–957.

Daston, G.P., Gooch, J.W., Breslin, W.J., Shuey, D.L., Nikiforov, A.I., Fico, T.A., Gorsuch, J.W., 1997. Environmental estrogens and reproductive health: a discussion of the human and environmental data. Reprod. Toxicol. 11, 465–481.

Harris, L.A., 2001. Differential equation models for the hormonal regulation of the menstrual cycle. Ph.D. Thesis, North Carolina State University, Raleigh, North Carolina. WEB site 〈www.lib.ncsu.edu/theses/available/etd-04222002-153727/unrestricted/etd.pdf〉.

Harris-Clark, L., Schlosser, P.M., Selgrade, J.F., 2003. Multiple stable periodic solutions in a model for hormonal control of the menstrual cycle. Bull. Math. Biol. 65, 157–173.

Hotchkiss, J., Knobil, E., 1994. The menstrual cycle and its neuroendocrine control. In: Knobil, E., Neill, J.D. (Eds.), The Physiology of Reproduction, second ed. Raven Press, Ltd., New York, pp. 711–750.

Jonard, S., Robert, Y., Cortet-Rudelli, C., Pigny, P., Decanter, C., Dewailly, D., 2003. Ultrasound examination of polycystic ovaries: Is it worth counting the follicles?. Hum. Reprod. 18, 598–603.

Keener, J., Sneyd, J., 2009. Mathematical Physiology I: Cellular Physiology, second ed Springer, New York.

McIntosh, J.E.A., McIntosh, R.P., 1980. Mathematical Modeling and Computers in Endocrinology. Springer, Berlin.

McLachlan, J.A., Korach, K.S., 1995. Symposium on estrogens in the environment, III. Environ. Health Perspect. 103 (Suppl. 7), 3–4.

McLachlan, R.I., Cohen, N.L., Dahl, K.D., Bremner, W.J., Soules, M.R., 1990. Serum inhibin levels during the periovulatory interval in normal women: relationships with sex steroid and gonadotrophin levels. Clin. Endocrinol. 32, 39–48.

Odell, W.D., 1979. The reproductive system in women. In: DeGroot, L.J. (Ed.), Endocrinology. Grune & Stratton, New York, pp. 1383–1400.

Ojeda, S.R., 1992. Female reproductive function. In: Griffin, J.E., Ojeda, S.R. (Eds.), Textbook of Endocrine Physiology second ed Oxford University Press, Oxford, pp. 134–188.

Pasteur, R.D., 2008. A multiple-inhibin model for the human menstrual cycle. Ph.D. Thesis, North Carolina State University, Raleigh, North Carolina. Web site 〈http://www.lib.ncsu.edu/theses/available/etd-06102008-194807/〉.

Pigny, P., Jonard, S., Robert, Y., Dewailly, D., 2006. Serum anti-Müllerian hormone as a surrogate for antral follicle count for definition of the polycystic ovary syndrome. J. Clin. Endocrin. Metab. 91, 941–945.

Plouffe Jr., L., Luxenberg, S.N., 1992. Biological modeling on a microcomputer using standard spreadsheet and equation solver programs: the hypothalamic-pituitary-ovarian axis as an example. Comput. Biomed. Res. 25, 117–130.

Reinecke, I., Deuflhard, P., 2007. A complex mathematical model of the human menstrual cycle. J. Theor. Biol. 247, 303–330.

Schlosser, P.M., Selgrade, J.F., 2000. A model of gonadotropin regulation during the menstrual cycle in women: qualitative features. Environ. Health Perspect. 108 (Suppl. 5), 873–881.

Schwartz, N.B., 1970. Cybernetics of mammalian reproduction. In: Gibian, H., Plotz, E.J. (Eds.), Mammalian Reproduction. Springer, Berlin, pp. 97–111.

Selgrade, J.F., Schlosser, P.M., 1999. A model for the production of ovarian hormones during the menstrual cycle. Fields Inst. Commun. 21, 429–446.

Welt, C.K., McNicholl, D.J., Taylor, A.E., Hall, J.E., 1999. Female reproductive aging is marked by decreased secretion of dimeric inhibin. J. Clin. Endocrinol. Metab. 84, 105–111.

Yen, S.S.C., 1999a. Polycystic ovarian syndrome (hyperandrogenic chronic anovulation). In: Yen, S.S.C., Jaffe, R.B., Barbieri, R.L. (Eds.), Reproductive Endocrinology. Physiology, Pathophysiology and Clinical Management fourth ed W.B. Saunders Co., Philadelphia, pp. 436–478.

Yen, S.S.C., 1999. The human menstrual cycle: neuroendocrine regulation. In: Yen, S.S.C., Jaffe, R.B., Barbieri, R.L. (Eds.), Reproductive Endocrinology. Physiology, Pathophysiology and Clinical Management fourth ed W.B. Saunders Co., Philadelphia, pp. 191–217.

Zeleznik, A.J., Benyo, D.F., 1994. Control of follicular development, corpus luteum function, and the recognition of pregnancy in higher primates. In: Knobil, E., Neill, J.D. (Eds.), The Physiology of Reproduction second ed Raven, New York, pp. 751–782.